Available online at www.sciencedirect.com
ScienceDirect
Energy Reports 7 (2021) 232–247
www.elsevier.com/locate/egyr

Tmrees, EURACA, 28 to 30 May 2021, Athens, Greece

Aromatic and aliphatic production of catalytic pyrolysis of lignin using ZSM-5/Al-SBA-15 catalyst derived from high-calcium fly ash

Supawan Vichaphund[a], Panida Wimuktiwan[a], Chakrit Soongprasit[a], Viboon Sricharoenchaikul[b], Duangduen Atong[a,*]

[a] National Metal and Materials Technology Center, National Science and Technology Development Agency, Pathumthani 12120, Thailand
[b] Department of Environmental Engineering, Faculty of Engineering, Chulalongkorn University, Bangkok 10330, Thailand

Received 27 July 2021; accepted 28 July 2021

Abstract

In this work, lignin was utilized as biomass feedstocks to study the feasibility of fuels and chemical production, while fly ash was used for synthesizing ZSM-5 (FA-ZSM-5) and SBA-15 (FA-SBA-15) catalysts for upgrading pyrolysis products. The use of fly ash offers several benefits such as reducing the fly ash disposal cost, solving environmental problems, and significantly increasing high valued products. Catalytic fast pyrolysis of kraft lignin using ZSM-5/ SBA-15 catalyst prepared from fly ash was studied using a pyrolysis-GC/MS system. The influence of temperature (400–600°C) during thermal pyrolysis, the FA-ZSM-5 and FA-SBA-15 ratios (1:0 ,2:1, 1:1, 1:2, 0:1), and lignin-to-catalyst ratios (1:5 and 1:10) on the hydrocarbon selectivity was investigated. Non-catalytic pyrolysis volatiles consisted of a high proportion of guaiacol compounds (G-type, 66.7%) and p-hydroxyl phenols (H-type, 18.0%). The presence of zeolite catalysts contributed to enhance both aliphatic and aromatic production, while a proportion of guaiacyl decreased significantly. The highest selectivity of aliphatic and aromatic HCs was achieved at feed to catalyst ratios of 1:10. Coupling HZSM-5 and Al-SBA-15 catalysts were more reactive in converting the alkoxy-phenol (G-type) and p-hydroxyphenyl compounds (P-type) toward both aliphatic HCs and monocyclic-aromatic HCs (MAHs), particularly benzene, toluene and xylene (BTX). Among all catalysts, FA-ZSM-5/ FA-SBA-15 ratio of 1:2 showed the optimum dual catalyst ratio to enhance the highest yield of aliphatic and aromatic hydrocarbons of 15.1 and 21.4 % with the acceptable yield of phenolic compounds (34%). ZSM-5/ SBA-15 catalyst prepared from fly ash showed high efficiency to convert solid lignin to MAHs (BTX). The decrease in the PAHs selectivity seemed to be good performing of this dual catalyst because it expected to decrease the coke formation on the catalyst surface.

Peer-review under responsibility of the scientific committee of the Tmrees, EURACA, 2021.

Keywords: Kraft lignin; ZSM-5; SBA-15; Phenolic compounds; Hydrocarbons

1. Introduction

Because of an alternative, clean and solely renewable carbon resource, the utilization of lignocellulosic biomass has been attracted growing attention to reduce a global fossil-fuel shortage and the environmental issues. Generally,

* Corresponding author.
E-mail address: duangdua@mtec.or.th (D. Atong).

https://doi.org/10.1016/j.egyr.2021.07.127

Peer-review under responsibility of the scientific committee of the Tmrees, EURACA, 2021.

Nomenclature

FA	Fly ash
ZSM-5	Zeolite Socony Mobil–5
SBA-15	Santa Barbara Amorphous-15
TGA	Thermogravimetric analysis
FTIR	Fourier transform infrared spectrophotometer
XRD	Powder X-ray diffraction
FESEM	Field emission scanning electron microscope
Py-GCMS	Pyrolysis gas chromatography mass spectrometry
H-unit	p-Hydroxyphenyl unit
G-unit	Guaiacyl unit
S-unit	Syringyl unit
MAHs	Monoaromatic hydrocarbons
PAHs	Polycyclic Aromatic Hydrocarbons

the three major constituents of biomass comprise of cellulose (30%–50%), hemicellulose (30%–40%), and lignin (20%–40%) [1,2]. Among biomass components, lignin is the most potential components to provide the abundantly renewable aromatic compounds. Two major processes provide a large amount of lignin by-products including the Kraft pulping of paper making producing lignin containing black liquor (∼50 million tons/years) and the bio-ethanol production. Lignin is a complex macromolecule, which is generally composed of three phenyl propane units (i.e. p-hydroxyphenyl (H-type), guaiacyl (G-type), and syringyl (S-type) connected through carbon–carbon and ether links [1,3,4]. Among the available conversion technologies, pyrolysis is one of the most promising and economic technologies in producing value-added fuels and chemicals. During lignin pyrolysis, lignin can be converted to phenolic compounds such as alkylphenols and methoxyphenols as well as aromatic hydrocarbons via several reactions involving deoxygenation (i.e. dehydration, decarbonylation, decarboxylation), demethoxylation, demethylation, dehydroxylation, and alkylation under moderate temperatures (400–600 °C) [5–7]. Phenolic compounds derived from lignin, particularly alkylphenols, can be valorized as green chemicals in the production of wood adhesives, detergents, stabilizers, polymers, resins, and pharmaceuticals, [6–8]. Meanwhile, green aromatic hydrocarbons (i.e. benzene, toluene, xylene) can be utilized as fuel components/additives and chemical intermediates. However, a low fraction of valuable products such as alkylphenols and aromatics are achieved during pyrolysis of lignin. Therefore, the use of catalysts in lignin pyrolysis contributes to efficiently enhance the conversion of methoxyphenol toward alkylphenols and aromatics.

Numerous catalysts have been applied for upgrading pyrolyzed vapors from lignin pyrolysis including microporous zeolites (HZSM-5, mordenite, Y-zeolite, X-zeolite, Beta) [1,3,9], mesoporous materials (SBA-15, MCM-41) [8,10] and metal oxides (MgO, Al_2O_3, ZrO_2, CaO, CoO/MoO_3) [4,10,11]. Among these catalysts, HZSM-5 has been proven to improve the maximum selectivity of aromatic hydrocarbons because an appropriate pore diameter and superior shape selectivity for providing the aromatization reaction as well as strong acidity [1,7,11]. However, the fast deactivation of HZSM-5 resulting from the coke formation on catalyst surface is a crucial problem [12,13]. Thus, to overcome this problem, the combination between microporous HZSM-5 and mesoporous materials can be applied to lessen polycyclic aromatic hydrocarbons (PAHs) leading to coke formation as well as improve the production of valuable chemicals.

The larger pore structure of mesoporous catalysts can facilitate the cracking and deoxygenation reactions of macromolecules to form smaller compounds into small compounds such as light phenols and aliphatic hydrocarbons. Consequently, the smaller molecules derived from lignin can react at the active sites inside HZSM-5 pore structure to obtain aromatic hydrocarbons via decarbonylation, decarboxylation, oligomerization, aromatization. Furthermore, coupling microporous zeolite and mesoporous materials contributed to reduce the side reactions of polymerization and polycondensation. As a result, polycyclic aromatic hydrocarbons (PAHs) can be inhibited, while the production of monocyclic aromatic hydrocarbons is increased significantly [7]. Several works studied on the employing dual catalysts in lignin pyrolysis to improve the yield of aromatic hydrocarbons as well as decrease PAHs formation as

shown in Table 1 [7,10,14,15]. Based on literatures and to our knowledge, there are no existing reports focusing on the use of integrating microporous HZSM-5 and mesoporous SBA-15 synthesized from high-calcium fly ash in catalytic pyrolysis.

The production of zeolite catalysts from fly ash offers several benefits including lowered disposal costs, reduced environmental impact, and resulting high valued products. Hence, this present work, lignin was utilized as biomass feedstocks to study the feasibility of fuels and chemical production. This research also aimed to utilize high-calcium fly ash as a raw material for synthesizing ZSM-5 (FA-ZSM-5) and Al-SBA-15 (FA-SBA-15). After synthesis process, catalytic fast pyrolysis of kraft lignin using ZSM-5/ SBA-15 catalysts prepared from fly ash was studied using an analytical pyrolysis-GC/MS. The effect of pyrolysis temperature (400–600 °C), the FA-ZSM-5 and FA-SBA-15 ratios (1:0, 2:1, 1:1, 1:2, 0:1), and lignin to catalyst ratios (1:5 and 1:10) on the hydrocarbon selectivity was investigated.

Table 1. The dual catalysts applied in catalytic pyrolysis of lignocellulosic biomass.

Dual catalyst	Catalyst preparation	Biomass feedstock	Reactor type	Catalyst ratios	Results	Ref.
HZSM-5 and Al-SBA-15	• Al-SBA-15 from sol–gel synthesis • Commercial ZSM-5	Lignin derived from corn cob wastes	Fixed-bed, 550 °C	Al-SBA-15:HZSM-5 ratios: 1:0, 3:1, 1:1, 1:3, 1:5, 0:1	• Both catalysts enhanced the MAHs production as well as inhibited the formation of PAHs • The optimum Al/SBA-15:ZSM-5 ratio was 1:3 • MAHs yield (mainly BTX) was 42.57%, while PAHs was reduced to 27.13%	[7]
(0%–50%) CaO and ZSM-5	• CaO prepared from commercial $CaCO_3$ • Commercial ZSM-5	Cellulose	Fixed-bed, 600 °C	(0%–50%) CaO:HZSM-5	• 15% CaO-85% ZSM-5 generated the maximum yield of olefin (5.59%) and aromatic HCs (13.42%)	[10]
CaO and HZSM-5	• Commercial CaO • ZSM-5 ($SiO_2/Al_2O_3 = 50$)	Hemicellulose and plastic	Py-GC/MS, 600 °C	CaO: HZSM-5 ratios: 1:0, 2:1, 1:1, 1:2, 0:1	• The highest yield of aromatic HCs (32%) was achieved at a CaO:HZSM-5 ratio = 1:2	[14]
Red mud and HZSM-5	• Red mud • Commercial HZSM-5 ($SiO_2/Al_2O_3 = 50$)	Organosolv lignin and polypropylene	TMR-GC/MS, 600 °C	Red mud:HZSM-5 ratio: 1:1	• Two-step RM and HZSM-5 showed the high aromatic formation (BTEX), while suppressing the PAHs	[15]

2. Experimental procedure

2.1. Raw materials and chemicals

The kraft lignin used through this study was procured from Sigma-Aldrich. Prior to experiment, the lignin sample with an irregular shape (Fig. 1(a)) was dried at 100 °C for 24 h. The elemental analysis (C, H, N, S) was performed by elemental analyzer (Model 628 series, Leco Corporation, USA), whereas oxygen (O) was determined by difference. The elemental composition of alkali lignin was C: 62.23%, H: 5.57%, N: 4.49%, O: 25.52%, and S: 1.79%, respectively. The thermogravimetric analysis of kraft lignin was investigated by using TGA/SDTA 851 (MettlerToledo). About 40–45 mg of each sample was heated from 50 °C to 900 °C under nitrogen atmosphere at a rate of 10 °C/min. Fourier transform-infrared spectroscopy (FT-IR) of kraft lignin were performed on a Perkin Elmer; Spectrum Spotlight 300. FTIR spectra was recorded in the region 400–4000 cm^{-1}.

The chemicals used in this experiment consisted of sodium metasilicate solution (Fluka, ≥97%), tetraethyl orthosilicate (TEOS, Merck, 98%), tetrapropylammonium bromide (TPABr, Aldrich, 98%), Pluronic P123 (M_w 5800, Sigma-Aldrich), sulfuric acid (Merck, 95%–97%), hydrochloric acid (Merck, 37%), and ammonium chloride (Sigma-Aldrich, ≥99.5%,).

A high-calcium fly ash was achieved from local power plants (Mae Moh power plant, Lampang) in Thailand. Prior to the synthesis process, the as-received fly ash was sieved through a 100-mesh screen (150 micron) to eliminate the large particles. Its chemical compositions determined by using XRF (X-ray fluorescence; Philips PW 2404) was

as follows: SiO_2, 28.5 wt%; CaO, 23.4 wt%; Fe_2O_3, 17.0 wt%; Al_2O_3, 16.1 wt%; SO_3, 7.37 wt%; MgO, 2.44 wt%; K_2O, 2.17 wt%; Na_2O, 1.72 wt%; TiO_2, 0.48 wt%; P_2O_5, 0.25 wt%; and LOI. 0.64 wt% [16,17]. From SEM image, the morphological form of fly ash mostly comprised of spherical shape with a smooth surface and a particle size less than 50 μm as demonstrated in Fig. 1(b).

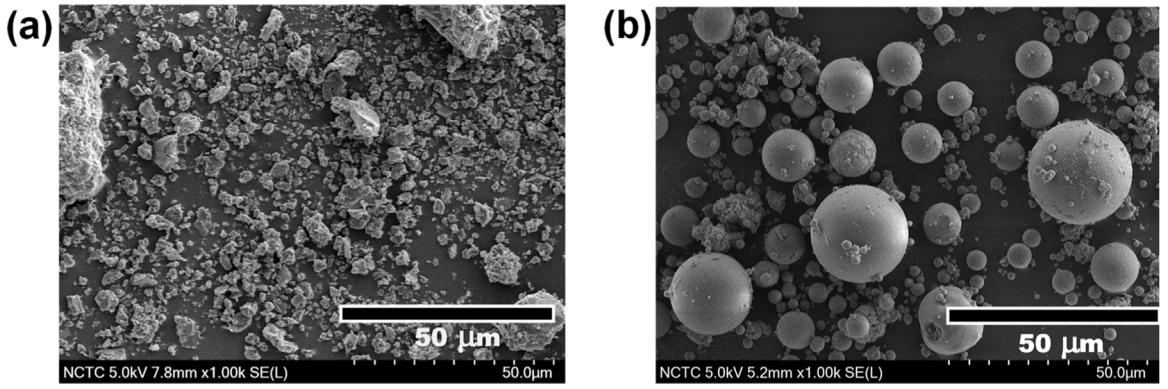

Fig. 1. Morphology of raw materials: (a) kraft lignin and (b) as-received fly ash.

2.2. Catalyst preparation

2.2.1. Synthesis of microporous ZSM-5: FA-ZSM-5

Microporous ZSM-5 derived from fly ash (FA-ZSM-5) was synthesized using fly ash via a conventional hydrothermal treatment according to literatures [18,19]. In this procedure, fly ash powder (approximately 2 g.) was initially dispersed in 3 M NaOH and then sodium metasilicate solution was added into the fly ash solution. After that, TPABr was added slowly to the mixture and stirred to obtain homogeneous mixture. Thereafter, conc. H_2SO_4 was applied to adjust the pH of the mixture. The molar ratio of compositions was in the following: $24SiO_2$:2.2TPABr:24.7 Na_2O:Al_2O_3:847.4 H_2O. After homogeneous mixing, the gel mixture was transferred to an autoclave to crystallize at 160 °C for 72 h under autogenous pressure. Then, the powder was separated, washed, dried at 100 °C overnight and heated at 540 °C for 5 h to remove template and impurities. The resulting solid material was consequently mixed with 1 M NH_4Cl solution at 80 °C for 8 h to obtain a HZSM-5 form. Then, the sample was filtered, washed, dried at 100 °C overnight, and heated at 540 °C for 5 h. The schematic of FA-HZSM-5 synthesis was displayed in Fig. S1.

2.2.2. Synthesis of mesoporous SBA-15 materials: FA-SBA-15

A hexagonally ordered mesoporous silica SBA-15 from fly ash (FA-SBA-15) was prepared according to a procedure in the literature by Soongprasit et al., 2020 [17]. Because of high CaO and Fe_2O_3 contents in as-received fly ash, the fly ash treatment with acid solution was firstly applied before the SBA-15 synthesis to eliminate the impurities. Initially, fly ash (about 10 g) was mixed with 1 M HCl solution (100 ml) in a solid and liquid ratio of 1:10 and continuously stirred at 90 °C for 1 h to obtain homogeneous mixture. Then, the acid treated-fly ash was separated, washed, and dried at 100 °C overnight. After that, acid treated-fly ash powder and sodium hydroxide were blended with a mass ratio of 1:1.2 and calcined at 550 °C for 1 h. To achieve the silicate–aluminate solution, the obtained solid was ground and mixed with deionized water (DI) in a mass ratio of 1:4. Then, Pluronic P123 (4.48 g, M_w = 5800, Sigma-Aldrich) and HCl solution were placed in a flask and stirred at 40 °C to obtain homogeneous mixture. After that, tetraethyl orthosilicate (4.8 g, Merck) and 32 ml of the supernatant were added to the P123 solution. Thereafter, the mixture was continuously stirred at 40 °C for 20 h. The mixture was poured into an autoclave and crystallized at 100 °C for 72 h. The white precipitate was then washed, oven-dried at 100 °C for 24 h and calcined in air at 550 °C for 6 h. The synthesis procedure of FA-SBA-15 was demonstrated in Fig.S2.

2.3. Catalyst characterization

The crystallization characteristics of FA-ZSM-5 sample was identified by using Powder X-ray diffractometer (XRD; PANalytical, X'Pert Pro, 40 kV, 45 mA) equipped with CuK α radiation. The XRD data of prepared sample was recorded at 2θ range of 5–55 °. Whereas the crystal structure of mesoporous FA-SBA-15 catalyst was determined by X-ray diffractometer (Rigaku TTRAX III, 50 kV, 300 mA) equipped with a CuK α source. The low-angle diffraction range was measured at $2\theta = 0.5$–5°. A field emission scanning electron microscope (FESEM; HITACHI, SU5000) was applied for investigating the morphology of catalysts. The surface area measurement and pore analysis were examined at −196 °C using a Autosorb-1 Quantachrome instrument. Before the adsorption experiment, both catalysts were evacuated at 300 °C for 8 h. From N_2 adsorption isotherm, the surface area was calculated via the Brunauer–Emmett–Teller (BET) model, whereas the pore volume was measured at P/P0 0.99.

2.4. Catalytic activity

Thermal and catalytic pyrolysis was conducted in a micro-pyrolyzer, PY-2020iD (Frontier Lab) equipped with an auto-shot sampler, AS-1020E (Frontier Lab). This micro-pyrolyzer unit was directly connected with a GC–MS detector, GCMS-QP2010 (Shimudzu). For lignin pyrolysis, about 400 μg of lignin sample was placed into a stainless-steel cup, loaded in a quartz reactor, and then pyrolyzed at 400–600 °C for 30 s. for exploring the influence of pyrolysis temperature. The effect of the catalyst involving the FA-ZSM-5/FA-SBA-15 ratios (1:0, 1:2, 1:1, 2:1, 0:1) and the lignin to catalyst weight ratio (1:5 and 1:10) were investigated. In a typical run, catalyst powder was placed above the lignin layer at the lignin to catalyst ratio of 1:5 and 1:10, respectively. After pyrolysis, the volatile components were collected for 30 s. before passing through the GC column. To separate the volatile compounds, a DB-1701 column (60 m × 0.25 mm, 0.25 μm film thickness) was applied with a 50:1 split ratio and a helium flow rate of 2.2 ml/min. The GC oven was programmed at 50 °C for 1 min, and then heated at 4 °C/min to 280 °C by a hold of 10 min. The mass spectrometer was recorded in the EI mode at 70 eV in 20–800 m/z range. In terms of identification and classification of volatile compounds, the NIST and Wiley mass spectral library was used. The micropyrolyzer-GC/MS set-up is shown in Fig. S3. Additionally, the selectivity of pyrolysis products was calculated according to the Eq. (1) [20]. The permanent gases (e.g., CO, CO_2, H_2, H_2O, $C_{1\text{-}3}$) cannot be separated or quantified by this GC set-up. To confirm the reproducibility of pyrolysis products, 15% standard deviation, the experiment was repeated three times.

$$Product\ selectivity\,(\%) = \frac{Area\ of\ the\ desired\ product}{Total\ area\ of\ the\ products} \times 100\% \tag{1}$$

2.5. Coke analysis

The amount of coke formation was measure by using TGA instrument using air as a carrier gas with a flow rate of 60 mL/min. The decomposition temperature of coke deposited on spent catalyst was programmed from 30 °C with a heating rate of 10 °C/min to 850 °C by a hold of 10 min. The relative of coke formation can be calculated according to the Eq. (2) [20].

$$\%Relative\ coke = \frac{m_{250\ ^\circ C} - m_{850\ ^\circ C}}{m_{250\ ^\circ C}} \times 100 \tag{2}$$

3. Results and discussion

3.1. Lignin characterization

The thermal degradation characteristics of kraft lignin determined by thermogravimetric analysis (TGA) under nitrogen atmosphere is shown in Fig. 2. The thermal decomposition of lignin occurred in three steps including the dehydration, the devolatilization and the carbonization. Firstly, a small change of weight loss at 50–150 °C can be observed owing to the evaporation of humidity. Meanwhile, a sharp decrease of weight loss, the rapid devolatilization, was found at 150–550 °C, corresponding to the major decomposition of lignin structure involving the cleavage of carbon–carbon and ether bond in the phenyl propane units (H, G, S) to form oligomers and

smaller compounds [21]. The last stage, carbonization stage up to 900 °C might be resulted from the degradation corresponded to the aromatization process of lignin fraction leading to high yield of solid char, ∼ 40.5%). Lazaridis et al. confirmed that the high residual char of 37.6% was obtained after pyrolysis kraft lignin at 800 °C [22]. Ma et al. suggested that this solid char resulted from amorphous aromatic ring in lignin converted into ordered graphite-like structure by polycondensation reaction [21].

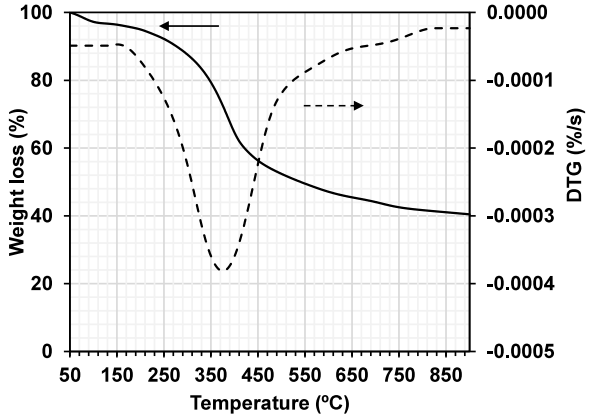

Fig. 2. Thermal degradation of the lignin sample in nitrogen atmosphere.

The FT-IR spectrum of alkali lignin is displayed in Fig. 3. A wide absorbance at 3410 cm^{-1} was attributed to –OH stretching vibration involving the presence of aliphatic and phenolic hydroxyl groups. Peaks at 2920 and 2851 cm^{-1} were assigned to C–H stretching of aliphatic structure (i.e., CH_2 and CH_3 groups). The vibration at 1597 and 1513 cm^{-1} were attributed to C–C stretching of aromatic structure. The band at 1371 cm^{-1} was related to –OH stretching of phenolic OH, whereas the vibration at 1327 cm^{-1} represented the C–O stretching of syrigyl ring (S-unit). The vibration signal at 1269, 1220 and 1126 cm^{-1} were assignable to C–O stretching and C–H aromatic of guaiacyl ring (G-unit). The strong band at 1031 cm^{-1} represented the aromatic C–H in plane deformation (G-unit > S-unit). The absorption band at 834 cm^{-1} corresponded to C–H aromatic related to syrigul (S-unit), while the absorbance at 619 cm^{-1} might correspond to sulfonic groups (S–C) remaining after the kraft pulping process [6,9,22,23].

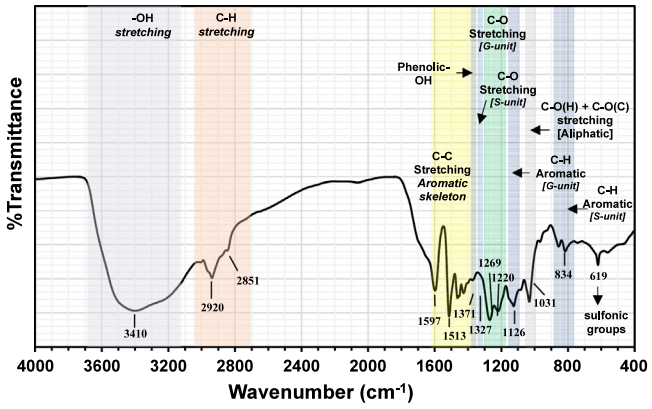

Fig. 3. FTIR spectrum of kraft lignin.

3.2. Physical–chemical characteristics of FA-ZSM-5 and FA-SBA-15

The XRD patterns and SEM micrographs of ZSM-5 and SBA-15 derived from fly ash are shown in Fig. 3. In case of ZSM-5 synthesized by conventional hydrothermal treatment (FA-ZSM-5, Fig. 4(a)), the sample revealed

well-resolved characteristic reflections of ZSM-5 diffraction peaks with 2θ at 7–9° and 23–25°, respectively. Unfortunately, small peak of wairakite (JCPDS: 89-0276) was detected as a minor phase owing to high amount of calcium in raw fly ash resulting in the reaction between aluminosilicate and calcium to form calcium aluminate silicate species [18,19]. The ZSM-5 formation consisted of three main steps including (1) the dissolution of fly ash with the alkali solution to obtain Si and Al species, (2) the condensation and nucleation of silicate and aluminate species in the presence of a polymeric template, and subsequently (3) the crystal growth on the outer surface of fly ash grains [9]. The morphology of FA-ZSM-5 particles revealed that the crystals were inter-grown with flat edge of the hexagonal face of the crystal with a size less than 5 μm as well as appeared in a large agglomeration. Generally, zeolite crystals derived from alternative sources (both natural clays and fly ash) are agglomerated compared to being separate when chemical reagent are used [24,25]. Fig. 4 (b) presents the low-angle XRD pattern of synthesized mesoporous FA-SBA-15 catalyst. Typically, the SBA-15 formation involves extracting the silicate species from fly ash and consequently hydrothermally treating the supernatant with the organic template (P123) to obtain a mesoporous SBA-15 material [17,26]. As a result, three characteristic diffraction peaks were found at $2\theta = 0.89°$, 1.53°, and 1.78°, which are typical peaks confirming the well-ordered mesoporous structure. The morphology of FA-SBA-15 particles are exhibited in Fig. 4(b). The SEM images demonstrated the well-defined rod-type structure with a particle size less than 5 μm. From these results, it clearly confirmed that the fly ash can be utilized as an alternative and inexpensive raw material for synthesizing both microporous ZSM-5 and SBA-15 mesoporous silica.

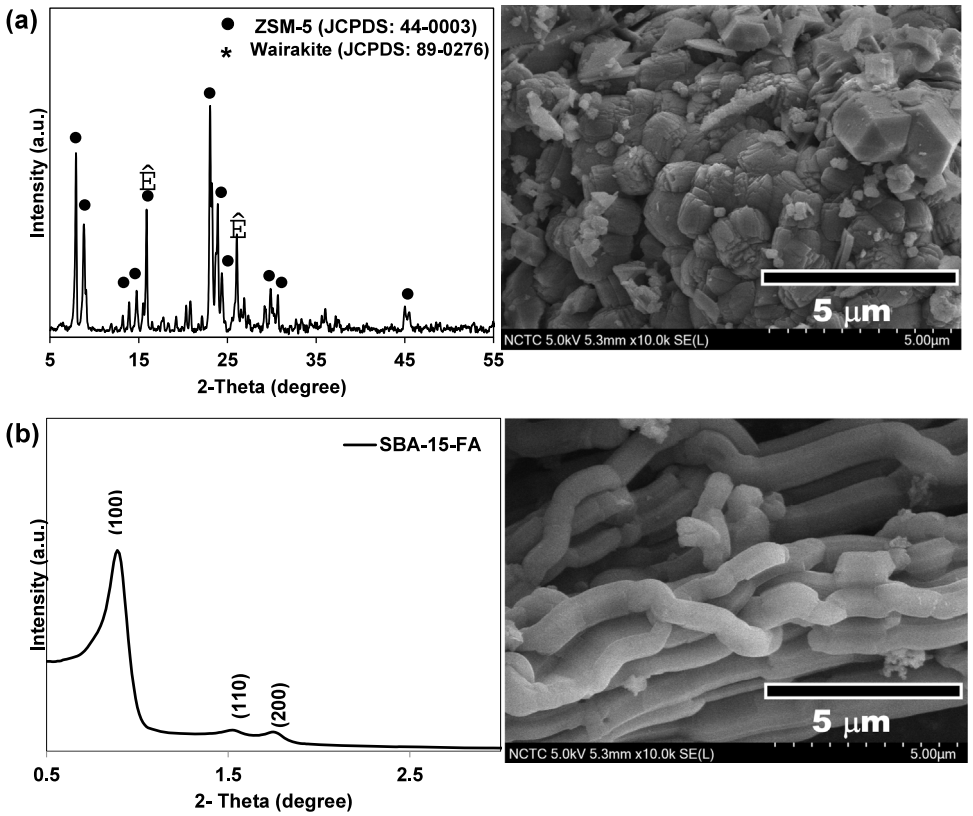

Fig. 4. XRD patterns and FE-SEM micrographs of (a) FA-HZSM-5 and (b) FA-SBA-15.

Fig. 5 The adsorption–desorption isotherms and pore size distribution (PSD) curves of FA-ZSM-5 and SBA-15-FA catalysts have been exhibited in Fig. 5, while the BET surface area and the porosity characteristics of both samples are listed in Table 2. The isotherm of FA-ZSM-5 had a type I isotherm with an H_4 type hysteresis loop at P/P0 higher than 0.4, associated with the micropore and mesopore in ZSM-5 structure. The combination between micropore and mesopore structures was exhibited by using the NLDFT method with a combination pore size range of <1 nm and 2–5 nm. The SBA-15-FA sample demonstrated a well-defined type IV isotherm with a H1 hysteresis

loop at P/P0 between 0.6 and 0.8, indicating the capillary condensation with uniform pores [27,28]. In addition, FA-SBA-15 catalysts demonstrated a single modal pore size distribution with narrow peak at centered approximately 5–7 nm. The surface textural properties of mesoporous FA-SBA-15 (S_{BET} = 705 m^2/g, V_{Tot} = 1.15 cm^3/g, and D avr = 6.56 nm) were found to be greater than those of microporous FA-ZSM-5 (S_{BET} = 207.5 m^2/g, V_{Tot} = 0.193 cm^3/g, and D avr = 3.72 nm). Wang et al. suggested that the higher surface area, greater pore volume and larger pore diameter of SBA-15 contributed to improve the efficiency of large molecular conversion during lignin pyrolysis [7].

Based on the results, the ZSM-5 and SBA-15 synthesized from fly ash exhibited the good properties including high purity, large surface area and pore volume, which are highly attractive for catalytic viewpoint.

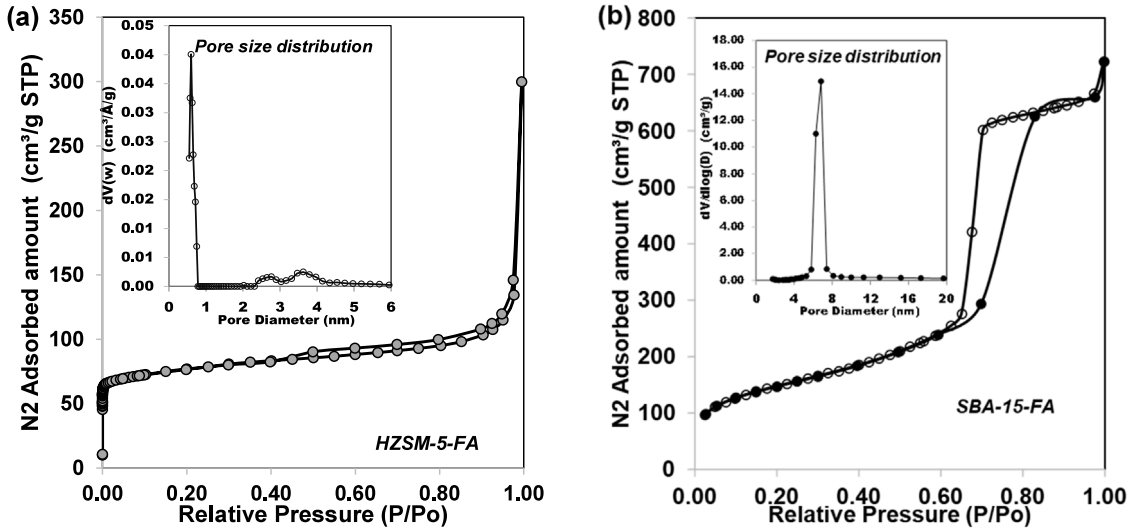

Fig. 5. Adsorption–desorption isotherms and PSD curves of (a) FA-HZSM-5 and FA-SBA-15.

Table 2. Textural properties and chemical composition of synthesized catalysts.

Sample	*FA-ZSM-5*	*FA-SBA-15*
Si/Al ratio	***44.46***[a]	***144.9***[b]
S $_{BET}$ (m^2/g)	207.5	702.2
S micropore area (m^2/g) (t-plot)	143.9	120.35
External SA (m^2/g) (t-plot)	63.55	581.85
Pore volume (cm^3/g)	0.193	1.152
V micro. (t-plot) (cm^3/g)	0.077	0.0462
V meso. (BJH method) (cm^3/g)	1.029	1.194
Pore diameter (nm)	3.72	6.56

[a]Determined by EDX.
[b]Determined by Micro-EDXRF.

3.3. Non-catalytic of kraft lignin

Non-catalytic pyrolysis of kraft lignin was conducted using Py-GC/MS system to investigate the effect of pyrolysis temperatures (400–600 °C) on the lignin pyrolysis behavior. The representative chromatograms at 400–600 °C as displayed in Fig. 6, whereas the identified compounds at these pyrolysis temperatures are listed in Table S1. The major organic components released from lignin pyrolysis can be divided into six groups including p-hydroxyphenyl units (H-type or phenol-type), guaiacyl (G-type), syringyl (S-type), aromatic hydrocarbons (Aromatics), aliphatic hydrocarbons (Aliphatics), and oxygenated compounds (Oxy.comp.: alcohols, aldehydes, acids, esters, ethers, ketones, and furans) as shown in Fig. 7.

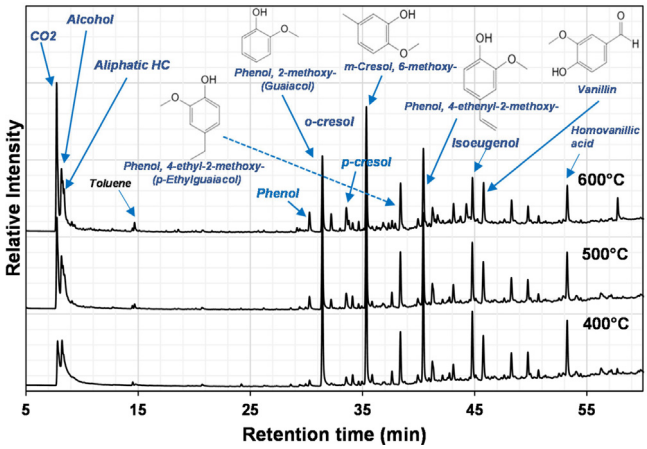

Fig. 6. The GC/MS chromatograms of kraft lignin pyrolyzed at 400–600 °C.

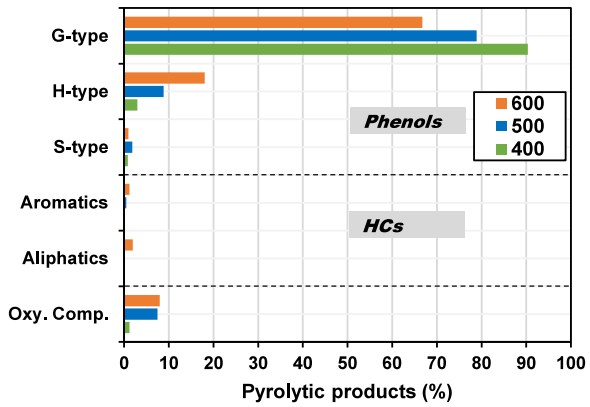

Fig. 7. Product selectivity (% area) of lignin pyrolyzed at 400–600 °C obtained from GC/MS.

A signal of carbon dioxide (CO_2) appeared at a retention time (RT) of 7.7 min, whereas methanol (CH_3OH) was observed at RT 7–8 min. The formation of CO_2 and methanol resulted from the decarboxylation, decarbonylation reaction and the cleavage of carbon–carbon bonds (5–5, β-1, and β-5) and ether links (α-O-4, β-O-4, and γ-O-4). Consequently, various substituent groups including hydroxyl (-OH), methyl (-CH_3) and methoxy (-OCH_3) began to separate from the phenylpropane structure and simultaneously permanent gases such as H_2O, CO, and CO_2 can be formed [21,23]. As the pyrolysis temperature increased, the peak intensity of carbon dioxide (CO_2) tended to increase gradually, corresponding to the degradation of heavy lignin molecules to form smaller phenolics involving p-hydroxyphenyl (H-type)), guaiacyl (G-type), syringyl (S-type) units [5].

As a result, the phenolic compounds were found as the major pyrolytic products, mostly guaiacol-type compounds including chiefly guaiacol (2-methoxy phenol), creosol, vanillin, 4-ethyl-2-methoxy phenol, and trans-isoeugenol (Fig. 6) that occurred at a retention time of 31–54 min. The guaiacyl unit has been exhibited as the major phenolic unit in softwood alkali lignin [6]. It was noticed that the high proportion of G-type phenols (78.9–90.4%) was found at lower temperature (400–500 °C) due to the breakage of β-O-4 bond [21], while a very low level of S-type phenols, 0.8–1.8%, was obtained at these pyrolysis temperatures. As the temperature increased from 400 to 600 °C the relative selectivity of guaiacol-type compounds (G-unit) drastically reduced from 90.39% to 66.75%. Meanwhile, the proportion of phenol-type compounds (H-unit) increased considerably from 2.95% at 400 °C to 18.02% at 600 °C, indicating that the higher pyrolysis temperature contributed to promote the demethoxylation reaction of both S-type and G-type leading to an increase content of H-type compounds [21,29,30]. These results were a good agreement with Kumar et al. who studied the non-catalytic soda lignin pyrolysis at 500–900 °C and found that

the guaiacol type compounds significantly reduced from 47.75% at 500 °C to 28.64% at 900 °C. Meanwhile, the phenol compounds was increased steadily from 6.05% at 500 °C to 16.42% at 900 °C [9]. Moreover, Lazaridis et al. investigated the thermal decomposition of kraft lignin at 400–600 °C and reported that the amount of alkoxy-phenols decreased, approximately 5%, while the alkyl-phenol compounds increased gradually (6%–7%) as pyrolysis temperature increased up to 600 °C [5].

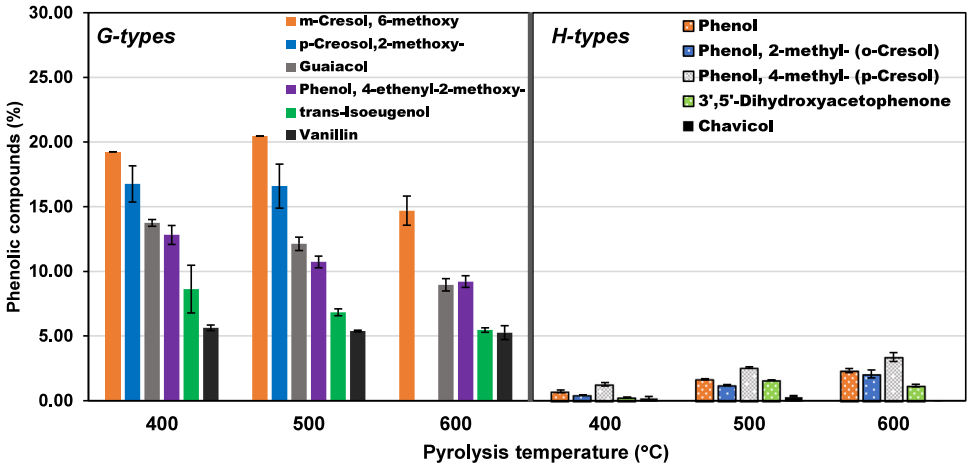

Fig. 8. Distributions of guaicol-types and phenol-types derived from kraft lignin pyrolysis.

The main compounds of H-type derived from kraft lignin pyrolysis (Fig. 8) were phenol, 2-methyl-phenol (o-cresol), 4-methyl-phenol (p-cresol), etc. Regarding other oxygenated compounds (i.e. aldehydes, esters, ethers, ketones, and furans), these compounds were generated due to the cracking reaction at side chains of lignin structure [1]. Their selectivity were found in small content and demonstrated slightly change with pyrolysis temperature. At highest pyrolysis temperature, 600 °C, a small content of light aliphatic (alkenes: C_5–C_6) and aromatic hydrocarbons (toluene) was found at RT between 8 and 15 min. The formation of toluene can be explained by the deoxygenation reactions such as the dehydroxylation and demethoxylation of the G-type and H-type phenolic compounds [21]. The formation of toluene was confirmed by Shao et al. They found that the production of toluene (0.95%) can be generated after kraft lignin pyrolyzed at high temperature of 650 °C via two reactions involving (i) block linkage cleavage of phenol-type (H-unit) and (ii) aromatic demethoxylation and dehydroxylation [29].

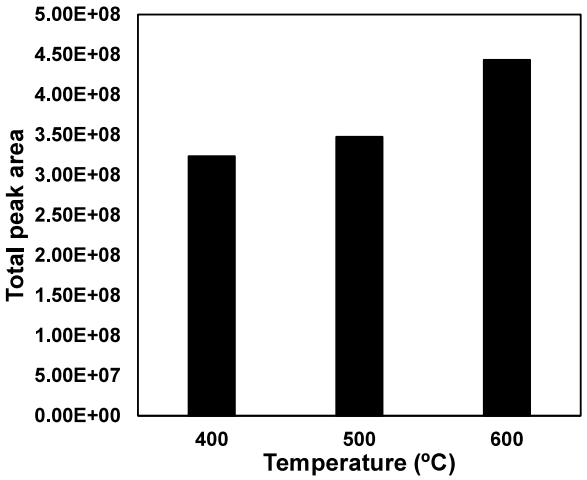

Fig. 9. The chromatographic peak areas obtained from lignin pyrolysis at 400–600 °C.

Based on these results, the maximum temperature (600 °C) promoted several reactions such as decarboxylation, demethoxylation, demethylation, dehydroxylation, and alkylation to achieve high yield of phenolic compounds as well as hydrocarbons including aromatics and aliphatics. This result is associated with the previous studies [6,7,21,29]. Additionally, the total chromatographic peak areas at the highest temperature (600 °C) exhibited a maximum proportion of volatile products owing to the enhancement of the secondary cracking reaction as displayed in Fig. 9. Therefore, a temperature of 600 °C was chosen to further examine the catalytic activity of dual catalysts.

3.4. Catalytic pyrolysis of lignin using FA-ZSM-5 and FA-SBA-15

The catalytic pyrolysis of kraft lignin using the combination between fly ash derived microporous HZSM-5 and mesoporous AlSBA-15 catalysts was studied using a micro-pyrolyzer-GC/MS system for improving the selectivity of phenol compounds and aromatic hydrocarbons as well as decreasing the coke formation. The effect of FA-ZSM-5 to FA-SBA-15 ratios (Z/S ratio of 1:0, 1:1, 1:2, 2:1 and 0:1) and lignin to catalyst ratios (L/C ratio of 1:5 and 1:10) on pyrolytic products was investigated.

The effect of different FA-ZSM-5 and FA-SBA-15 ratios (1:0, 1:1, 1:2, 2:1 and 0:1) on the product yields and lignin to catalyst ratios (1:5 and 1:10) pyrolyzed at 600 °C were investigated to assess the capability of the microporous and mesoporous catalysts in terms of enhancing the hydrocarbon selectivity (aromatic and aliphatic hydrocarbons) as well as reducing the undesirable products such as larger oxygenated compounds and PAHs. The catalytic pyrolysis of lignin with pure FA-ZSM-5 (1:0) or FA-SBA-15 (0:1) was conducted as a reference. As shown in Fig. 10, the selectivity of pyrolytic products after catalytic run had differed considerably from thermal run (lignin).

With the lignin to catalyst ratios of 1:5 as shown in Fig. 10(a), the presence of FA-ZSM-5 (Z/S of 1:0) reduced the proportion of guaiacol compounds (G-type) considerably from 66.7% (thermal) to 50.3%, whereas S-type compounds was completely eliminated through the cracking reactions and dehydration at external acid site of ZSM-5 surface [9,31]. Thus, the fraction of phenol compounds (H-type) increased gradually from 18.0% to 22.9% because of the enhancement of the conversion of methoxy phenols (including G-type and S-type) through particularly demethoxylation reaction. In guaiacol, C_{Ar}-OCH_3 (356 kJ/mol) demonstrated lower bond energy than C_{Ar}-OH (414 kJ/mol) facilitating more removal of methoxyl groups bonded to lignin structure. Consequently, the higher proportion of methoxyl-free phenols was obtained [1]. Additionally, a few of oxygenated compounds (alcohols, ketones, aldehydes, esters) of 5.3% and furans of 2.1% were obtained due to the cracking reaction of side-chain in lignin structure [9].

As a result, the selectivity of hydrocarbons including aliphatics and aromatics, increased significantly from 1.9% to 5.7% for aliphatics and from 1.2 to 11.1% for aromatics, respectively. In terms of aromatic hydrocarbons, the oxygenated volatiles derived from lignin entered in the selective pore structure of ZSM-5 and underwent

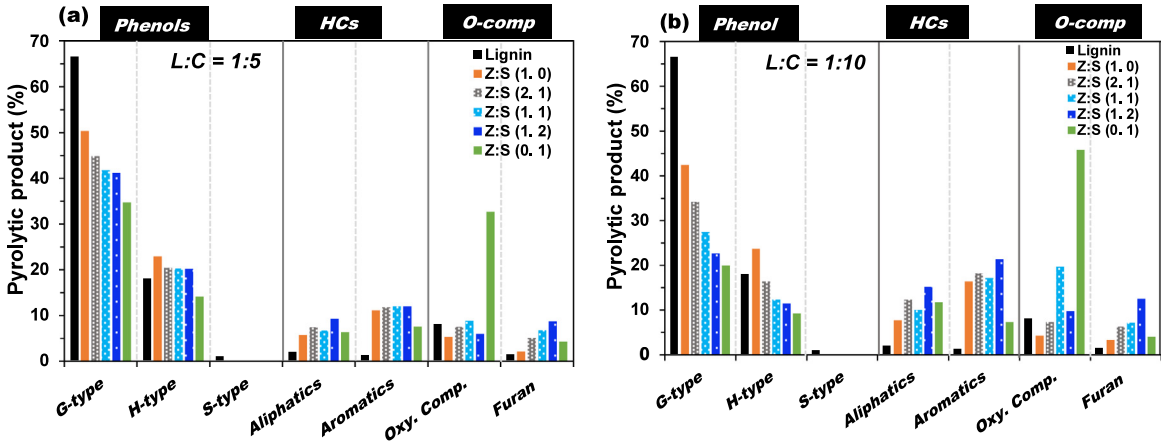

Fig. 10. Pyrolytic products in CFP of kraft lignin with FA-HZSM-5 and FA-Al/SBA-15 using lignin to catalyst ratios: (a) 1:5 and (b) 1:10.

several reactions comprising of decarbonylation, decarboxylation, dehydration, demethoxylation, dehydroxylation, demethylation and aromatization at the active sites to generate H_2O, CO_2, CH_3OH, light phenols, aliphatic as well as aromatic hydrocarbons [1,6,7,9]. The ability of microporous ZSM-5 to promote the aromatic compounds was suggested by Lazaridis et al. They examined the catalytic fast pyrolysis (CFP) of kraft lignin using HZSM-5 (40) and the lignin to HZSM-5 ratio of 1:4 at 600 °C and found that the application of HZSM-5 catalyzed the transformation of lignin oligomers to aromatics, mainly toluene, benzene, and xylene, approximately 40% [5]. This result was also consistent with Kumar, et al. who applied the commercial ZSM-5 (Si/Al ∼ 30–40) to promote the conversion of large oxygenates derived from soda lignin pyrolysis to aromatics. The significant increase of aromatic selectivity (particularly, BTX) of 21.66% was achieved when using ZSM-5 at pyrolysis temperature of 600 °C [9].

Unlike microporous ZSM-5, the larger pore size (6.56 nm) and greater pore volume (1.15 cm^3/g) of SBA-15 facilitated the dehydration and cracking reactions of heavier oxygenates into smaller molecules such as light phenols, and aliphatic compounds through a series of reactions including demethylation, demethoxylation, H-abstraction and side-chain breaking reaction of mesoporous SBA-15 molecular sieves [7]. Thus, pure FA-SBA-15 achieved higher conversion efficiencies of heavy methoxyphenols, particularly guaiacol compounds (G-type, 34.7%), during catalytic lignin pyrolysis than did the FA-ZSM-5 through the demethoxylation reaction to form smaller phenols due to the mild acidity and the spatial configuration of SBA-15. Although, the lowest fraction of phenol compounds (H-type, 14.1%) was produced in the presence of fly ash derived-SBA-15 catalyst, the partial oxygenates can be upgraded to form both aliphatic (6.4%) and aromatic hydrocarbons (7.6%) via a side chain breaking and reforming reactions as well as oligomerization. This corresponded with the findings of a previous reported by Jeon et al. who studied the catalytic conversion of lignin over Al-SBA-15 and observed that the small amounts of aromatic hydrocarbons (7%–8%) were produced through depolymerization and olefin oligomerization of lignin derived volatiles when using mesoporous Al-SBA-15 with a pore size of 10.7 nm, surface area of 429 m^2/g and pore volume of 1.13 cm^3/g [32]. Wang et al. investigated the catalytic conversion of lignin extracted from corn cob wastes using ZSM-5 and SBA-15 catalysts and found that the phenolic compounds (44.83%) and aliphatic hydrocarbons (19.83%) exhibited as predominant pyrolytic products generating by the Al-SBA-15 catalyst [7]. However, the high proportion of other oxygenates (i.e. aldehydes, alcohols, carboxylic acids, esters, ketones, and furans) was observed when using FA-SBA-15 catalyst. This might be resulted from the coke deposition on the surface of SBA-FA as shown in Table 3. Using pure FA-SBA-15 showed higher amount of coke formation than using other catalysts at the lignin:catalyst ratio of 1:5.

In terms of the synergistic effect of HZSM-5 and SBA-15, the combination of both microporous FA-ZSM-5/mesoporous FA-SBA-15 with different Z/S ratios (1:1, 1:2, and 2:1) was investigated. Under different FA-ZSM-5/FA-SBA-15 ratios, the fraction of guaiacol compounds (G-type) decreased substantially (41.2–44.8%), whereas the yields of phenol class compounds (H-type) increased gradually (20.2–20.4%). The integration between FA-ZSM-5 and FA-SBA-15 catalysts promoted both formation of smaller species such as light phenols and aliphatic hydrocarbons by demethoxylation, demethylation, and side-chain cleavage as well as enhanced the deoxygenation reactions and aromatization leading to aromatic hydrocarbons. Hence, the production of aliphatic (6.7–9.3%) and aromatic hydrocarbons (11.8%–12%) was higher than that of the FA-HZSM-5 or FA-SBA-15 run. The maximum selectivity of hydrocarbons (21.3%) was obtained with a low oxygenated content (14.7%) at an FA-ZSM-5/FA-SBA-15 ratio of 1:2.

With the highest catalyst content (L/C ratio of 1:10, Fig. 10(b)), a higher amount of catalyst greatly improved the selectivity of desirable pyrolytic products compared to a lower amount of catalyst (L:C = 1:5). Coupling HZSM-5 and Al-SBA-15 catalysts resulted in the effective conversion of the alkoxy-phenol (G-type) and p-hydroxyphenyl compounds (P-type) toward both aliphatics and monocyclic aromatics (MAHs), particularly benzene, toluene and xylene (BTX). This indicated that the high amounts of active sites in the presence of FA-ZSM-5 as well as the larger pore structure of FA-SBA-15 promoted the effective conversion of lignin-derived oxygenates to form light phenolic compounds, aliphatic and aromatic HCs.

In case of HZSM-5, the formation of aromatic hydrocarbons can be explained by two mechanism including hydrocarbon pool and phenolic pool mechanism. For hydrocarbon pool mechanism, the light phenolic species (i.e. phenol and alkylphenols) can react at the active sites inside HZSM-5 pore structure to obtain aromatic hydrocarbons through a sequence of reactions involving cracking, decarboxylation, decarbonylation, oligomerization, and aromatization. Another mechanism, the small phenolic compounds can be changed to form phenolic precursors in the phenolic pool via several reactions such as transalkylation, isomerization, and condensation. These precursors

can be further converted to aromatic hydrocarbon by cracking and H-transfer reaction [7,9,20,31]. With regarding to mesoporous SBA-15, this mesopore catalyst had a limitation for producing the aromatic hydrocarbon due to its mild acidity, larger pore diameter and greater external surface area. Thus, mesoporous SBA-15 has more ability to promote the conversion of macromolecular lignin-derived oxygenates into small molecules such as light phenolic compounds and aliphatic HCs, which is consistent with the findings of literatures [7,17,32]. In the presence of integrating FA-ZSM-5/FA-SBA-15, the production of phenolic compounds was then decreased to 22.6–34.6% and 11.5–16.4% for G-type and P-type. As a result, the aliphatic and aromatic selectivity increased significantly to 10.0–12.3% and 17.2–21.4%, respectively.

Among all catalysts, FA-ZSM-5/ FA-SBA-15 ratio of 1:2 showed the optimum dual catalyst ratio to increase the highest yield of aliphatic and aromatic HCs of 15.1 and 21.4% with the acceptable yield of phenolic compounds (34%). Phenol and its derivatives can be utilized as chemical precursors for the production of chemical products as well as resins. Hydrocarbons including aliphatics and aromatics are valuable products, which can be further extracted as fine chemicals and fuel additives [17,20,32,33]. Additionally, the selectivity of oxygenates (alcohols, aldehydes, ketones, esters, furans) tended to increase slightly as the function of FA-SBA-15 content. Furan compounds significantly increased after catalysis from 1.4% (non-catalytic) to 12.5%. Unfortunately, a lower selectivity of phenolic compounds (G-type of 19.9% and H-type of 9.2%) and hydrocarbons (19.02%) was obtained when using FA-SBA-15 catalyst (Z:S (0:1)). Thus, the higher yield of oxygenated compounds was observed noticeably. The most abundant oxygenate compounds detected in the pyrolysis vapors were acetic acid (16.12%) and acetone (11.31%). The increase in the undesirable oxygenates might be resulted from the formation of coke covering on the external surfaces of catalyst as well as blocking into mesopore of SBA-15 structure leading to the decrease in catalytic efficiency [17,20]. This result corresponded to the amount of coke accumulation on the surface of the used catalysts as shown in Table 3.

It was noticed that a significant reduction of coke covering on the surface or blocking within the pore structure was found when using higher catalyst content. This result corresponded to Fan et al. who stated that the increase in catalyst loading amount reduced the coke deposition on the surface of catalyst, meanwhile higher catalytic temperature contributed to promote the decomposition of coke [1]. At this ratio, the amount of coke accumulation produced from the mesoporous fly ash derived-SBA-15 (FA-SBA-15) was considerably high (9.71%) as compared to other catalysts. Interestingly, the lowest coke formation of spent FA-ZSM-5 was achieved, 5.3%, which was attributed to higher acidity and suitable pore structure leading to the reduction of coke deposition as well as the desirable compound enrichment such as light phenols, aliphatics and aromatics. In case of the incorporation between FA-ZSM-5 and FA-SBA-15 catalysts, a FA-ZSM-5 and FA-SBA-15 ratio of 1:2 showed lesser the amounts of coke (7.16%) deposited on the surface/into pore structure compared with other ratios.

Table 3. The coke formation of used catalysts after pyrolyzed at 600 °C.

Lignin: Catalyst ratio	ZSM-5:SBA-15 ratios	Coke (%)
1:5	Z:S (1:0)	9.45
	Z:S (2:1)	14.34
	Z:S (1:1)	10.31
	Z:S (1:2)	14.79
	Z:S (0:1)	24.14
1:10	Z:S (1:0)	5.30
	Z:S (2:1)	9.40
	Z:S (1:1)	9.88
	Z:S (1:2)	7.16
	Z:S (0:1)	9.71

Fig. 11 demonstrated the selectivity of hydrocarbon compounds including linear aliphatics (C_5–C_{10}, C_{11}–C_{15}), cyclic aliphatics (C_5–C_{10}), monocyclic-aromatic HCs (MAHs) and polycyclic-aromatic HCs (PAHs). In terms of aliphatic-HC, all catalysts favored to promote the production of light linear aliphatics (C_5–C_{10}) such as alkenes and alkanes, while heavy linear aliphatics (C_{11}–C_{15}) and cyclic hydrocarbons (C_5–C_{10}) such as cycloalkanes and cycloalkenes were found in small content. The addition of mesoporous SBA-15 catalysts remarkably improved the proportion of aliphatic HCs. In case of the aromatic hydrocarbons, the major aromatic hydrocarbons were mainly MAHs involving benzene (C_6), toluene (C_7), ethylbenzene (C_8), and xylene (o-xylene and m-xylene: C_8)

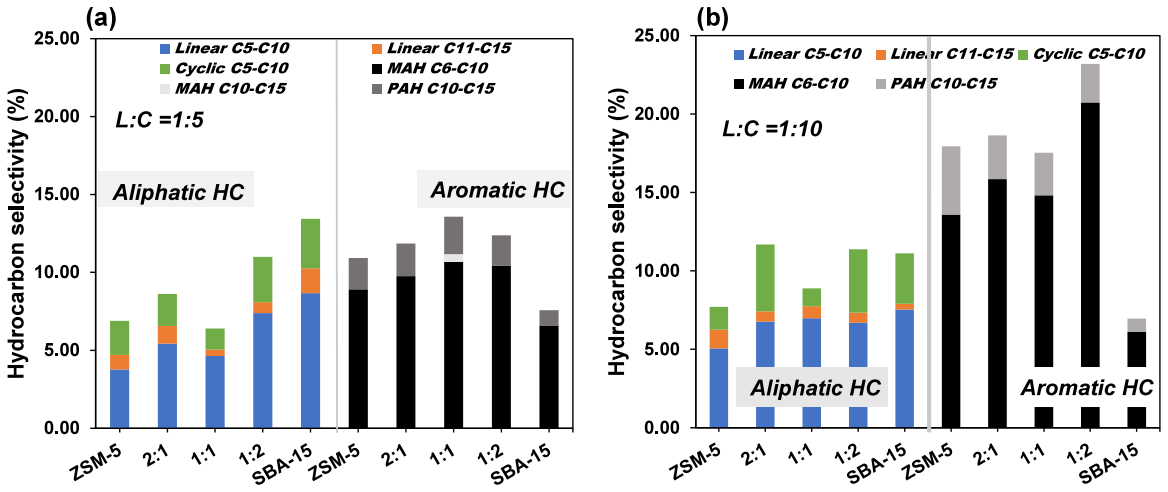

Fig. 11. Distribution of aliphatics and aromatics of the kraft lignin with FA-HZSM-5 and FA-SBA-15 using L/C ratios of (a) 1:5 and (b) 1:10.

(BTX), indicating that the MAHs can be possibly generated at catalytic active site inside the pore structure [7,31]. These aromatic HCs were classified in the gasoline range (C_5–C_{12}) and were consistent with the previous works [1,17.18,20]. BTX compounds are well known as valuable chemical precursors for improving octane number.

At lignin to catalyst ratios of 1:5 (Fig. 11(a)), the MAHs selectivity (C_6–C_{15}) was in the following order of Z1:S1 (11.18%) > Z1:S2 (10.42%) > Z2:S1 (9.77%) >FA-ZSM-5 (8.91%) > FA-SBA-15 (6.56%). While the formation of PAHs was produced in range of 1.01%–2.39%. The low level of both MAHs and PAHs formation generated from FA-SBA-15 might be due to large pore volume and mild acidity, limiting the ability of aromatic formation as well as hindering the molecular diffusion [20]. Consequently, the highest level of aliphatic fraction, particularly linear hydrocarbons (C_5–C_{10}), occurred when using pure FA-SBA-15. These results suggested that a combination of FA-ZSM-5 and FA-SBA-15 catalysts can encourage a high level of MAHs formation with a low PAHs production.

However, at higher lignin-to-catalyst ratios of 1:10 (Fig. 11(b)), the polycyclic aromatic hydrocarbons (PAHs) were also generated as the content of FA-SBA-15 increased. The PAHs selectivity levels (C_{10}–C_{15}) were as followed: FA-ZSM-5 (4.36%) > Z2:S1 (2.79%) ~ Z1:S1 (2.72%) > Z1:S2 (2.45%) > FA-SBA-15 (less than 1%). FA-ZSM-5 catalysts effectively increased the PAHs formation as compared to other catalysts. The formation of PAHs inside a pore structure of ZSM-5 was reported by Yu et al. who investigated the application of ZSM-5 in CFP of lignin with the lignin: catalyst ratio of 1:20. They found that the pore dimension of microporous ZSM-5 can be expanded to approximately 8.1–8.3 Å at high temperature, 650 °C, and hence, PAHs such as naphthalenes was possibly produced inside the pore structure of ZSM-5 [31]. The PAHs can be occurred from the polymerization and condensation of PAH compounds leading to the coke formation covering on the surface or blocking inside pore structure.

From these results, it can be concluded that both pore structure and acidity of zeolites influenced the conversion of oxygenates to light phenols and hydrocarbons remarkably. Pore size influenced the mass transfer and diffusion of lignin-derived oxygenates into pore, meanwhile the acidity of zeolites significantly enhances the formation of aliphatics and aromatics. Higher catalyst content (L/C = 1:10) is important factor to increase catalytic active sites and surface area, providing more effective in converting primary pyrolysis vapors by deoxygenation and aromatization reactions leading to the production of valuable aromatic and aliphatic hydrocarbons. Additionally, the synergetic effect of ZSM-5 and SBA-15 derived from fly ash with an appropriate ratio (Z1:S2) contributed to enhance aliphatic and aromatic selectivity with the ability to alleviate PAH formation causing catalyst deactivation. Thus, ZSM-5 and SBA-15 derived from fly ash can be valorized in the lignin pyrolysis for hydrocarbon and phenolic compound conversion.

4. Conclusions

The FA-ZSM-5 and FA-SBA-15 catalysts can be successfully prepared from high calcium fly ash. The surface textural properties of mesoporous FA-SBA-15 (S_{BET} = 705 m^2/g, V_{Tot} = 1.15 cm^3/g, and D avr = 6.56 nm) were

found to be greater than those of microporous FA-ZSM-5 (S_{BET} = 207.5 m^2/g, V_{Tot} = 0.193 cm^3/g, and D avr = 3.72 nm). A highest amount of catalyst (L/C ratio of 1/10) greatly improved the selectivity of desirable pyrolytic products compared to a lower amount of catalyst (L/C ratio of 1/5). Coupling HZSM-5 and Al-SBA-15 catalysts resulted in the effective conversion of the alkoxy-phenol (G-type) and p-hydroxyphenyl compounds (P-type) toward both aliphatics and monocyclic aromatics (MAHs), particularly BTX. Among all catalysts, FA-ZSM-5/ FA-SBA-15 ratio of 1:2 showed the optimum dual catalyst ratio to increase the highest yield of aliphatic and aromatic HCs of 15.1 and 21.4% with the acceptable yield of phenolic compounds (34%). Additionally, the synergetic effect of ZSM-5 and SBA-15 derived from fly ash with an appropriate ratio (Z1:S2) contributed to enhance the production of aliphatic and aromatic HCs with the ability to alleviate PAH formation. Thus, ZSM-5 and SBA-15 derived from fly ash can be valorized in the lignin pyrolysis for hydrocarbon and phenolic compound conversion.

Declaration of competing interest

The authors declare that they have no known competing financial interests or personal relationships that could have appeared to influence the work reported in this paper.

Acknowledgment

This research was supported by the National Metal and Materials Technology Center, Thailand [Project No. MT-ICF-61-POL-07-593-I].

Appendix A. Supplementary data

Supplementary material related to this article can be found online at https://doi.org/10.1016/j.egyr.2021.07.127.

References

[1] Fan L, Chen P, Zhou N, Liu S, Zhang Y, Liu Y, et al. In-situ and ex-situ catalytic upgrading of vapors from microwave-assisted pyrolysis of lignin. Bioresour Technol 2018;247:851–8. http://dx.doi.org/10.1016/j.biortech.2017.09.200.
[2] Paysepar H, Venkateswara Rao KT, Yuan Z, Shui H, Xu C. Production of phenolic chemicals from hydrolysis lignin via catalytic fast pyrolysis. J Anal Appl Pyrolysis 2020;149:104842. http://dx.doi.org/10.1016/j.jaap.2020.104842.
[3] Fan L, Ruan R, Li J, Ma L, Wang C, Zhou W. Aromatics production from fast co-pyrolysis of lignin and waste cooking oil catalyzed by HZSM-5 zeolite. Appl Energy 2020;263:114629. http://dx.doi.org/10.1016/J.APENERGY.2020.114629.
[4] Mullen CA, Boateng AA. Catalytic pyrolysis-GC/MS of lignin from several sources. Fuel Process Technol 2010;91(11):1446–58. http://dx.doi.org/10.1016/J.FUPROC.2010.05.022.
[5] Lazaridis PA, Fotopoulos AP, Karakoulia SA, Triantafyllidis KS. Catalytic fast Pyrolysis of Kraft Lignin with Conventional, Mesoporous and Nanosized ZSM-5 Zeolite for the production of Alkyl-Phenols and Aromatics. Front Chem 2018;6:295. http://dx.doi.org/10.3389/fchem.2018.00295.
[6] Supriyanto, Usino DO, Ylitervo P, Dou J, Sipponen MH, Richards T. Identifying the primary reactions and products of fast pyrolysis of alkali lignin. J Anal Appl Pyrolysis 2020;151:104917. http://dx.doi.org/10.1016/j.jaap.2020.104917.
[7] Wang S, Li Z, Yi W, Fu P, Zhang A, Bai X. Renewable aromatic hydrocarbons production from catalytic pyrolysis of lignin with Al-SBA-15 and HZSM-5: Synergistic effect and coke behaviour. Renew Energy 2021;163:1673–81. http://dx.doi.org/10.1016/j.renene.2020.10.108.
[8] Shafaghat H, Lee HW, Yang L, Oh D, Jung S-C, Rhee GH, et al. Catalytic co-conversion of Kraft lignin and linear low-density polyethylene over mesoZSM-5 and Al-SBA-15 catalysts. Catal Today 2020;355:246–51. http://dx.doi.org/10.1016/j.cattod.2019.04.052.
[9] Kumar A, Kumar A, Kumar J, Bhaskar T. Catalytic pyrolysis of soda lignin over zeolites using pyrolysis gas chromatography-mass spectrometry. Bioresour Technol 2019;291:121822. http://dx.doi.org/10.1016/j.biortech.2019.121822.
[10] Yang M, Shao J, Yang H, Zeng K, Wu Z, Chen Y, et al. Enhancing the production of light olefins and aromatics from catalytic fast pyrolysis of cellulose in a dual-catalyst fixed bed reactor. Bioresour Technol 2019;273:77–85. http://dx.doi.org/10.1016/j.biortech.2018.11.005.
[11] Ryu HW, Lee HW, Jae J, Park Y-K. Catalytic pyrolysis of lignin for the production of aromatic hydrocarbons: Effect of magnesium oxide catalyst. Energy 2019;179:669–75. http://dx.doi.org/10.1016/j.energy.2019.05.015.
[12] Santana JA, Carvalho WS, Ataíde CH. Catalytic effect of ZSM-5 zeolite and HY-340 niobic acid on the pyrolysis of industrial kraft lignins. Ind Crops Prod 2018;111:126–32. http://dx.doi.org/10.1016/j.indcrop.2017.10.023.
[13] Wang S, Li Z, Bai X, Yi W, Fu P. Catalytic pyrolysis of lignin in a cascade dual-catalyst system of modified red mud and HZSM-5 for aromatic hydrocarbon production. Bioresour Technol 2019;278:66–72. http://dx.doi.org/10.1016/j.biortech.2019.01.037.
[14] Ding K, Zhong Z, Wang J, Zhang B, Fan L, Liu S, et al. Improving hydrocarbon yield from catalytic fast co-pyrolysis of hemicellulose and plastic in the dual-catalyst bed of CaO and HZSM-5. Bioresour Technol 2018;261. http://dx.doi.org/10.1016/j.biortech.2018.03.138.
[15] Ryu HW, Kim DH, Jae J, Lam SS, Park ED, Park Y-K. Recent advances in catalytic co-pyrolysis of biomass and plastic waste for the production of petroleum-like hydrocarbons. Bioresour Technol 2020;310:123473. http://dx.doi.org/10.1016/j.biortech.2020.123473.

[16] Vichaphund S, Sricharoenchaikul V, Atong D. Selective aromatic formation from catalytic fast pyrolysis of Jatropha residues using ZSM-5 prepared by microwave-assisted synthesis. J Anal Appl Pyrolysis 2019;141:104628. http://dx.doi.org/10.1016/j.jaap.2019.104628.
[17] Soongprasit C, Aht-Ong D, Sricharoenchaikul V, Vichaphund S, Atong D. Hydrocarbon production from catalytic pyrolysis-GC/MS of Sacha Inchi residues using SBA-15 Derived from Coal Fly Ash. Catalysts 2020;10(9):1031. http://dx.doi.org/10.3390/catal10091031.
[18] Vichaphund S, Aht-Ong D, Sricharoenchaikul V, Atong D. Characteristic of fly ash derived-zeolite and its catalytic performance for fast pyrolysis of jatropha waste. Environ Technol 2014;35(17):2254–61. http://dx.doi.org/10.1080/09593330.2014.900118.
[19] Soongprasit K, Vichaphund S, Sricharoenchaikul V, Atong D. Activity of Fly Ash-derived ZSM-5 and Zeolite X on fast Pyrolysis of Millettia (Pongamia) Pinnata Waste. Waste Biomass Valoriz 2020;11(2):715–24. http://dx.doi.org/10.1007/s12649-019-00709-7.
[20] Vichaphund S, Wimuktiwan P, Sricharoenchaikul V, Atong D. In situ catalytic pyrolysis of jatropha wastes using ZSM-5 from hydrothermal alkaline fusion of fly ash. J Anal Appl Pyrolysis 2019;139:156–66. http://dx.doi.org/10.1016/j.jaap.2019.01.020.
[21] Ma Z, Wang J, Zhou H, Zhang Y, Yang Y, Liu X, et al. Relationship of thermal degradation behavior and chemical structure of lignin isolated from palm kernel shell under different process severities. Fuel Process Technol 2018;181:142–56. http://dx.doi.org/10.1016/j.fuproc.2018.09.020.
[22] Tejado A, Peña C, Labidi J, Echeverria JM, Mondragon I. Physico-chemical characterization of lignins from different sources for use in phenol–formaldehyde resin synthesis. Bioresour Technol 2007;98(8):1655–63. http://dx.doi.org/10.1016/j.biortech.2006.05.042.
[23] Soongprasit K, Sricharoenchaikul V, Atong D. Phenol-derived products from fast pyrolysis of organosolv lignin. Energy Rep 2020;6:151–67. http://dx.doi.org/10.1016/j.egyr.2020.08.040.
[24] Ríos RCA, Williams CD, Roberts CL. A comparative study of two methods for the synthesis of fly ash-based sodium and potassium type zeolites. Fuel 2009;88(8):1403–16. http://dx.doi.org/10.1016/j.fuel.2009.02.012.
[25] Mohiuddin E, Isa YM, Mdleleni MM, Sincadu N, Key D, Tshabalala T. Synthesis of ZSM-5 from impure and beneficiated Grahamstown kaolin: Effect of kaolinite content, crystallisation temperatures and time. Appl Clay Sci 2016;119:213–21. http://dx.doi.org/10.1016/j.clay.2015.10.008.
[26] Dindi A, Quang DV, Vega LF, Nashef E, Abu-Zahra MRM. Applications of fly ash for CO2 capture, utilization, and storage. J CO2 Util 2019;29:82–102. http://dx.doi.org/10.1016/j.jcou.2018.11.011.
[27] Kumar P, Mal N, Oumi Y, Yamana K, Sano T. Mesoporous materials prepared using coal fly ash as the silicon and aluminium source [10.1039/B104810B]. J Mater Chem 2001;11(12):3285–90. http://dx.doi.org/10.1039/B104810B.
[28] Akti F. Effect of kaolin on aluminum loading success in synthesis of Al-SBA-15 catalysts: Activity test in ethanol dehydration reaction. Microporous Mesoporous Mater 2020;294:109894. http://dx.doi.org/10.1016/j.micromeso.2019.109894.
[29] Shao L, Zhang X, Chen F, Xu F. Fast pyrolysis of Kraft lignins fractionated by ultrafiltration. J Anal Appl Pyrolysis 2017;128:27–34. http://dx.doi.org/10.1016/j.jaap.2017.11.003.
[30] Yu J, Wang D, Sun L. The pyrolysis of lignin: Pathway and interaction studies. Fuel 2021;290:120078. http://dx.doi.org/10.1016/j.fuel.2020.120078.
[31] Yu Y, Li X, Su L, Zhang Y, Wang Y, Zhang H. The role of shape selectivity in catalytic fast pyrolysis of lignin with zeolite catalysts. Appl Catal A 2012;447–448:115–23. http://dx.doi.org/10.1016/j.apcata.2012.09.012.
[32] Jeon M-J, Jeon J-K, Suh DJ, Park SH, Sa YJ, Joo SH, et al. Catalytic pyrolysis of biomass components over mesoporous catalysts using Py-GC/MS. Catal Today 2013;204:170–8. http://dx.doi.org/10.1016/j.cattod.2012.07.039.
[33] Wang J, Zhong Z, Ding K, Li M, Hao N, Meng X, et al. Catalytic fast co-pyrolysis of bamboo sawdust and waste tire using a tandem reactor with cascade bubbling fluidized bed and fixed bed system. Energy Convers Manage 2019;180:60–71. http://dx.doi.org/10.1016/j.enconman.2018.10.056.